Polymer Journal (2016) 48, 509–515

www.nature.com/pj

ORIGINAL ARTICLE

Controlled incorporation behavior of gold nanoparticles into ABC triblock terpolymer with double-helical morphology

Takeshi Higuchi[1], Hidekazu Sugimori[2,3], Hiroshi Yabu[1] and Hiroshi Jinnai[1]

Control of the incorporation behavior of Au nanoparticles grafted with polystyrene (PS) in an ABC triblock terpolymer composed of PS, polyisoprene (PI) and poly(methyl methacrylate) (PMMA) with double-helical morphology was investigated by transmission electron microtomography and three-dimensional structural analysis. The assemblies in the microdomains were controlled by varying the molecular weight of the PS molecules grafted on the Au nanoparticles. For PS-grafted Au nanoparticles >0.3 times the domain dimension of the PS microdomain in the poly(styrene-*b*-isoprene-*b*-methyl methacrylate) (SIM) film, the nanoparticles were located at the center of the PS microdomains to minimize the entropy loss of the PS segment of SIM. In contrast, Au nanoparticles <0.2 times the domain dimension adsorbed preferentially to the interface of the PS and PI microdomains to reduce the interfacial tension between the nanoparticles and SIM. Intermediate-sized Au nanoparticles were uniformly distributed in the PS microdomains. The distribution of PS-grafted Au nanoparticles was explained by the entropic and enthalpic gains in the microdomains.
Polymer Journal (2016) **48,** 509–515; doi:10.1038/pj.2016.19; published online 17 February 2016

INTRODUCTION

Block copolymers are composed of different polymer segments connected via covalent bonds and spontaneously form ordered nanoscale structures. Various types of microphase-separated structures (for example, spherical, cylindrical, lamellar and double gyroid structures in diblock copolymers) are formed depending on the volume fraction of the polymer segments.[1,2] The periodic length of a microphase-separated structure depends on the total molecular weight of the block copolymer. Recent developments in polymerization techniques have allowed various types of block copolymers (for example, star,[3,4] graft,[5] multiblock[6] and gradient block copolymers[7,8]) to be synthesized, resulting in the formation of very complicated periodic nanoscale structures. These diverse microphase-separated structures are now used in various applications such as separation filters,[9] photonic crystals,[10,11] laser devices[12] and templates for etching in lithography.[13,14]

Incorporating inorganic nanoparticles into polymer matrices is an important strategy for creating new materials.[15] These hybrid materials, often called nanocomposites, exhibit excellent properties such as high mechanical strength, electron conductivity, catalytic activity and optical and magnetic properties. Owing to the morphological diversity of block copolymers, incorporating inorganic nanoparticles into microphase-separated domains has attracted a great deal of attention.[16] Various methods have been proposed to introduce inorganic nanoparticles into microdomains,[17–21] some of which exploit the surface affinity of nanoparticles in order to control their location in microdomains.[22,23]

Microphase-separated diblock copolymers were initially used as a nanoscale template for inorganic nanoparticles,[16,24–26] and later multiblock copolymers such as triblock terpolymers were also used owing to their rich variety of three-dimensional (3D) morphologies.[27–30] Recently, Li *et al.*[31] reported successful introduction of Au and Pt nanoparticles into a double-gyroid structure of an ABC linear triblock terpolymer. ABC triblock terpolymers exhibit more complicated and intriguing 3D morphologies. Depending on the volume fraction of polymer segments, 'cylinders-on-cylinder' and 'helices-on-cylinder' morphologies were formed that consisted of cylinders or helices of B polymer formed on the surface of A polymer cylinders in the C polymer matrix.[28,29] Using these structures as templates to accommodate nanoparticles may produce nanocomposites with great potential as electromagnetic wave absorbers and metamaterials.[32]

We have reported the morphological control of the helices-on-cylinder morphology formed by ABC linear triblock terpolymers composed of polystyrene (PS), polybutadiene and poly(methyl methacrylate) (PMMA).[33,34] Transmission electron microtomography

[1]Institute of Multidisciplinary Research for Advanced Materials (IMRAM), Tohoku University, Sendai, Japan and [2]Department of Polymer Science and Engineering, Kyoto Institute of Technology, Kyoto, Japan
[3]Current address: Fuel Cell Cutting-Edge Research Center Technology Research Association, Tokyo, Japan.
Correspondence: Professor H Jinnai, Institute of Multidisciplinary Research for Advanced Materials (IMRAM), Tohoku University, 2-1-1, Katahira, Aoba-ku, Sendai, Miyagi 980-8577, Japan.
E-mail: hjinnai@tagen.tohoku.ac.jp
Received 3 December 2015; revised 8 January 2016; accepted 16 January 2016; published online 17 February 2016

(TEMT) was used for 3D structural analyses of the complicated morphologies.[35–37] The observations revealed that the helices-on-cylinder morphology was composed of polybutadiene helical microdomains around hexagonally packed PS cylindrical cores in a PMMA matrix. In our previous studies, we controlled the number of helical strands (two, three and four strands), the pitch of helices and the orientation of helices to the substrate.[34,38] In the present study, we demonstrated that Au nanoparticles grafted with PS molecules were selectively introduced into the microdomains of ABC linear triblock terpolymers composed of PS, polyisoprene (PI) and PMMA by changing the molecular weight of the PS on the surface of Au nanoparticles.

EXPERIMENTAL PROCEDURE

Materials

Tetraoctyl ammonium bromide (C8H17NBr) was purchased from Sigma-Aldrich (St Louis, MO, USA). Hydrogen tetrachloroaurate(III) tetrahydrate ($HAuCl_4 \bullet 4H_2O$) and sodium tetraborohydride ($NaBH_4$) were purchased from Wako Pure Chemical Co., Inc. (Tokyo, Japan). Poly(styrene-*b*-isoprene-*b*-methyl methacrylate) (SIM) and thiol-terminated polystyrenes (PS-SH) with three different molecular weights were purchased from Polymer Source, Inc. (Dorval, QC, Canada). The molecular characteristics of the polymers used in this study are summarized in Table 1. All solvents in this study were purchased from Wako Pure Chemical Co., Inc. All reagents were used as received without further purification.

Synthesis of PS-grafted Au nanoparticles

Au nanoparticles were prepared by a two-phase liquid–liquid system according to a modified literature procedure.[39] An aqueous solution (20 ml) of $HAuCl_4$ (20.6 mg, 0.05 mmol) was prepared in a conical beaker (200 ml). A toluene solution of C8H17NBr (82.0 mg, 0.15 mmol) was added to the solution with stirring until all $HAuCl_4$ was transferred into the organic phase. A toluene solution (20 ml) of the PS-SH (150 mg, 0.05 mmol) was added to the organic phase, and then aqueous $NaBH_4$ (10 ml, 189 mg, 5.0 mmol) was added dropwise. The solution changed from yellow to red. After stirring for 2 h, the organic phase was collected and extracted with toluene three times, and then the solvent was concentrated to several ml in a rotary evaporator. To remove excess PS-SH, ethanol (50 ml) was added and the precipitate was collected by decantation. The crude product was washed with ethanol three times by ultrasonication and centrifugation (12 000 r.p.m. for 15 min at 5 °C). The purified product was dried *in vacuo* to remove the solvents completely.

Preparation of SIM films incorporated with Au nanoparticles grafted with PS chains

The dried Au nanoparticles grafted with PS molecules were redispersed in chloroform ($CHCl_3$). The hybrid films were prepared by casting 5 wt% $CHCl_3$ solutions of SIM containing the Au nanoparticles at weight concentrations (ϕ_{Au}) of 30 and 50 wt%. The resulting films were exposed to saturated $CHCl_3$ vapor for 2 days at 24 °C, and then $CHCl_3$ was evaporated by nitrogen gas at a flow rate of 5 ml min^{-1}.

The hybrid films were embedded in a photocurable acrylic resin, and then irradiated with visible light (wavelength: $\geqq$400 nm). The cured resin blocks were microtomed to a thickness of ~100 nm by using an ultramicrotome (EM UCT, Leica Microsystems GmbH, Germany) with a diamond knife at room temperature. The ultrathin sections were transferred onto Cu mesh grids with supporting polyvinyl formal membranes. The sections were stained with RuO_4 for 3 min, and then with OsO_4 for several hours to visualize the PS and PI phases, respectively, in the microphase-separated structures of SIM. Finally, Au nanoparticles 5 nm in diameter (British Biocell International, Cardiff, UK) were deposited on the back of the supporting membranes.

TEM and TEMT observations

Transmission electron microscopy (TEM) and TEMT (JEM-1200EX, JEOL, Co., Ltd, Tokyo, Japan) were performed at 100 kV, and the system was equipped with a slow-scan CCD camera (Gatan USC 2000, Gatan Inc., Pleasanton, CA, USA). A series of TEM images were acquired at tilt angles of $\pm 60°$ in 1° step. The TEM images were aligned by the fiducial marker method with Au nanoparticles deposited on a supporting membrane. After the alignment, the tilt series of the TEM images were reconstructed by a filtered back projection algorithm.[40]

RESULTS AND DISCUSSION

Synthesis of PS-grafted Au nanoparticles

A typical TEM image of Au nanoparticles grafted with PS-SH-11k is shown in Supplementary Figure S1a. The Au nanoparticles were observed, whereas the PS molecules on the Au nanoparticles were not visualized in the TEM image because of their low electron density. The average diameter of the Au nanoparticles (d_{AuNP}) was measured as 3.2 nm in the TEM images (Supplementary Figure S1b). The synthesized Au nanoparticles in this experiment, including Au nanoparticles grafted with other PSs, had similar Au core diameters, as summarized in Table 2. Because the grafted PS molecules were not clearly observed in the TEM images, the whole diameters (D) of Au nanoparticles containing the grafted PS molecules were calculated according to the literature[41](Table 2).

Hybrid films of SIM and Au-11k

The microphase-separated structure of the neat SIM film was determined by TEM and TEMT before incorporation of the Au nanoparticles (Supplementary Figure S2). SIM forms a double-helical structure of PI around hexagonally packed cylinders of PS in a PMMA matrix. The diameters of the PI and PS domains were 11 ± 1 and 30 ± 4 nm, respectively. TEM images of the SIM films incorporated with Au-11k nanoparticles at $\phi_{Au} = 30$ and 50 are shown in Figures 1a and e, respectively. To determine the 3D structures of the hybrid films, the films in the regions enclosed in black squares in Figures 1a and e were observed by TEMT. The sliced images from the reconstructed images in the xy and xz planes are shown in Figures 1b, c, f and g, where the z axis corresponds to the direction of the electron beam. In the reconstructed images, small black dots are Au-11k nanoparticles. With respect to the microphase-separated structure of SIM, gray, black and white regions are attributed to PS, PI and PMMA domains, respectively, because the PS and PI segments are stained with RuO_4 and OsO_4, respectively. When the Au-11k nanoparticles were incorporated into the SIM films at $\phi_{Au} = 30$, and the nanoparticles were

Table 1 Molecular characteristics of polymers

Name	M_n(S/I/M) (kg mol^{-1})	M_w/M_n	*Volume fractions (S/I/M)*
SIM	58/22/330	1.10	0.20/0.09/0.71
PS-SH-11k	11.5/–/–	1.08	1.0/–/–
PS-SH-3k	3/–/–	1.07	1.0/–/–
PS-SH-1k	1/–/–	1.40	1.0/–/–

Abbreviations: PS-SH, thiol-terminated polystyrene; SIM, poly(styrene-*b*-isoprene-*b*-methyl methacrylate).

Table 2 Diameters of Au nanoparticles

Name	d_{AuNP} (nm)[a]	D (nm)[b]
Au-11k	3.2	1.6
Au-3k	2.7	8.2
Au-1k	3.3	6.2

[a]Diameter of Au nanoparticles measured in transmission electron microscopy (TEM) images.
[b]Polystyrene (PS) chains on Au nanoparticles were calculated for a conical conformation.[41]

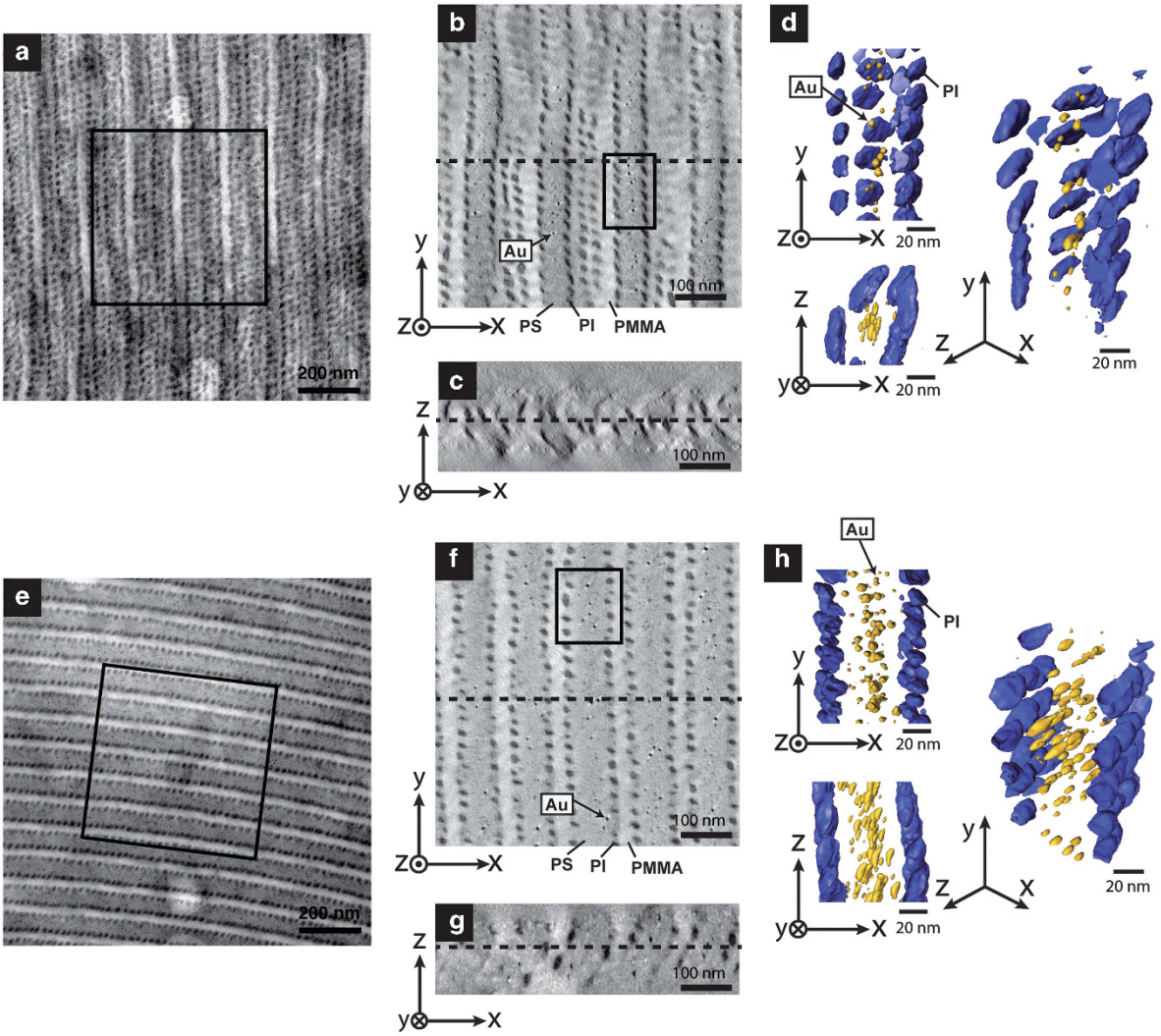

Figure 1 Transmission electron microscopy (TEM) and three-dimensional (3D) structures of poly(styrene-*b*-isoprene-*b*-methyl methacrylate) (SIM) films incorporated with Au-11k nanoparticles. (**a**) TEM image, and reconstructed images in region enclosed by the black square in (**a**) digitally sliced in the (**b**) xy and (**c**) xz planes of SIM films incorporated with Au-11k nanoparticles at $\phi_{Au} = 30$. (**d**) The 3D structures of polyisoprene (PI) and Au nanoparticles from three directions visualized from the region enclosed by the black square in (**b**). (**e**) TEM image, and reconstructed images in the region enclosed by the black square in (**e**) digitally sliced in the (**f**) xy and (**g**) xz planes of SIM films incorporated with Au-11k nanoparticles at $\phi_{Au} = 50$. (**h**) The 3D structures of PI and Au nanoparticles from three directions visualized from the square region of (**f**).

observed in the PS microdomains. The 3D structures of PI microdomains and Au nanoparticles in the region enclosed by a black square in Figure 1b are shown in Figure 1d. The PI microdomains and Au nanoparticles are visualized as blue and yellow, respectively. The 3D structure revealed that spherical PI domains were formed around the PS cylinders and Au nanoparticles were located in the center of the PS cylinders. However, in the films incorporated with Au-11k nanoparticles at $\phi_{Au} = 50$, a lamellar structure of PS and PMMA was formed and the Au nanoparticles were located at the center of PS layers, as shown in Figure 1h. The result indicates that a morphological transition of the microphase-separated structure of SIM was induced by incorporating Au-11k nanoparticles.

Hybrid films of SIM and Au-3k

To prevent the morphological transition of microphase-separated structures of SIM by incorporating Au nanoparticles, PS molecules with a lower molecular weight than PS-SH-11k were grafted onto Au nanoparticles. As shown in Table 2, the average and whole diameter of Au-3k nanoparticles were $d_{AuNP} = 2.7$ and $D = 8.2$ nm, respectively. The size of Au core was similar to that of the Au-11k nanoparticles, whereas the whole size of Au-3k nanoparticles was approximately half that of the Au-11k nanoparticles. Figure 2 shows the TEM image (Figure 2a), reconstructed images (Figures 2b and c) and 3D structures (Figure 2d) of the SIM films incorporated with Au-3k nanoparticles at $\phi_{Au} = 30$. Figure 2d clearly shows that the double-helical morphology of the PI phases was retained on the PS cylinders, although the PI phases were partially disconnected. The Au-3k nanoparticles were incorporated into the center of the PS cylinders and also near the interfaces between PS and either PI or PMMA. When the concentration of Au-3k nanoparticles was increased to $\phi_{Au} = 50$, the microphase-separated structures of SIM disappeared and the macrophase separation between SIM and Au-3k nanoparticles occurred as shown in Supplementary Figure S3.

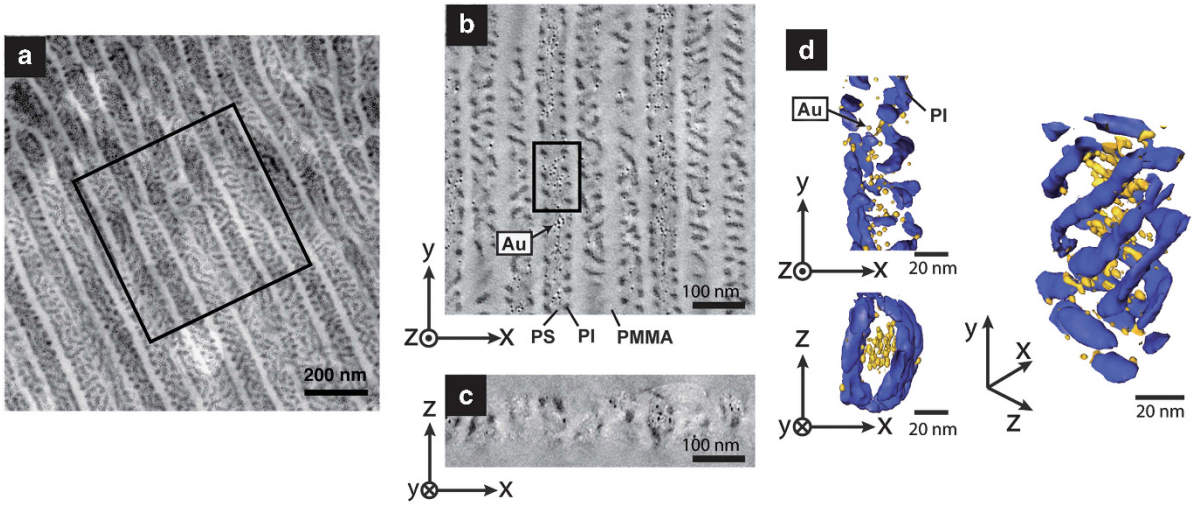

Figure 2 Transmission electron microscopy (TEM) and three-dimensional (3D) structures of poly(styrene-*b*-isoprene-*b*-methyl methacrylate) (SIM) films incorporated with Au-3k nanoparticles. (**a**) TEM image, and reconstructed images in the region enclosed by the black square in (**a**) digitally sliced in the (**b**) xy and (**c**) xz planes of SIM films incorporated with Au-3k nanoparticles at $\phi_{Au} = 30$. (**d**) The 3D structures of polyisoprene (PI) and Au nanoparticles from three directions visualized from the square region of (**b**).

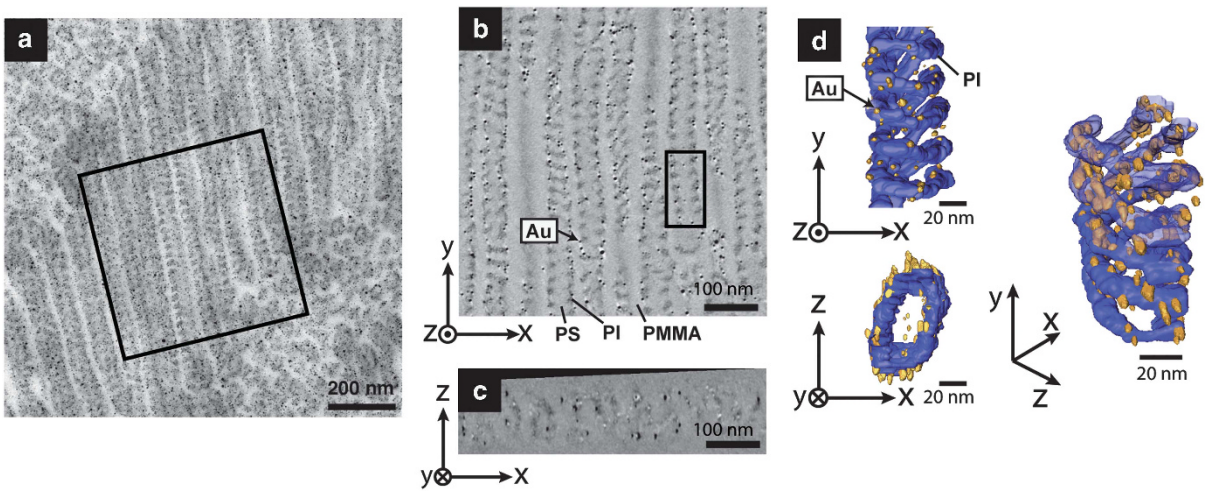

Figure 3 Transmission electron microscopy (TEM) and three-dimensional (3D) structures of poly(styrene-*b*-isoprene-*b*-methyl methacrylate) (SIM) films incorporated with Au-1k. (**a**) TEM image, and reconstructed images in region enclosed by the black square in (**a**) digitally sliced in the (**b**) xy and (**c**) xz planes of the SIM films incorporated with Au-1k at $\phi_{Au} = 50$. (**d**) The 3D structures of polyisoprene (PI) and Au nanoparticles from three directions visualized from the square region of (**b**).

Hybrid films of SIM and Au-1k

The Au nanoparticles grafted with PS-SH-1k, which has a lower molecular weight than PS-SH-3k, were incorporated into the SIM films. Compared with the Au-3k nanoparticles, the Au-1k nanoparticles had a similar Au core diameter ($d_{AuNP} = 3.3$) and a smaller whole diameter ($D = 6.2$ nm). Figure 3 shows the TEM image (Figure 3a), reconstructed images (Figures 3b and c) and 3D structures (Figure 3d) of the SIM films incorporated with Au-1k nanoparticles at $\phi_{Au} = 50$. The 3D structures obtained with TEMT revealed that the PI phases formed double-helical structures on the PS cylinders even at $\phi_{Au} = 50$. It is also remarkable that many Au-1k nanoparticles were located near the interfaces between the PS and PI phases (Au-11k nanoparticles were located in the PS and PI microdomains), although the Au nanoparticles were grafted with the PS molecules.

Incorporation behaviors of Au nanoparticles in microphase-separated structures of SIM

The localization mechanism of the nanoparticles grafted with polymer molecules in the microphase-separated structures has been studied theoretically[42] and experimentally.[43–45] The relative size of nanoparticles to the domain spacing of microphase-separated structure is a major factor governing the localization of the incorporated nanoparticles. A simulation of Au nanoparticle localization in the microdomain predicted that small particles with sizes of $D/L < 0.2$ would be located at the interfaces of microdomains, whereas large particles with sizes of $D/L > 0.3$ would be located near the center of the microdomains to minimize the entropy loss of the block copolymer segment, where D is the particle diameter including grafted polymers on the nanoparticles, and L is the dimension of the microdomain.[42]

Bockstaller *et al.*[46] reported that the theoretical prediction is in good agreement with the experimental results.

To consider the entropic effect on localization of Au nanoparticles in the microphase-separated structures of SIM, *D*/*L* values of Au-11k, Au-3k and Au-1k were calculated to be 0.53, 0.27 and 0.21, respectively (Table 3). According to the theory described above,[42] the Au-11k nanoparticles tend to segregate at the center of PS microdomain (Figure 4a). Because Au-3k nanoparticles have an intermediate value of *D*/*L* between 0.3 and 0.2, they would uniformly distribute in the PS microdomains (Figure 4b). The theory predicts that the Au-1k nanoparticles ($D/L \sim 0.2$) would be located at the interfaces between the microdomains of either PS/PI or PS/PMMA. The experimental results are in good agreement with the theoretical predictions.

For the nanoparticles located at the interfaces of the microdomains, an interfacial tension (that is, enthalpic energy) among the nanoparticles and polymer segments is also important in addition to the entropic effect. The absorption energy (E_a) is defined as follows:[45,47]

$$\frac{E_a}{k_B T} = \frac{\pi R^2 \gamma_{A-B}}{k_B T}(1 - |cos\theta_{A-B}|)^2$$
$$|cos\theta_{A-B}| = \frac{|\gamma_{NP-A} - \gamma_{NP-B}|}{\gamma_{A-B}} = \frac{\Delta\gamma}{\gamma_{A-B}} \quad (1)$$

where R is the nanoparticle radius, γ_{A-B} is the interfacial tension between A and B segments of the AB diblock copolymer and γ_{NP-A} or γ_{NP-B} is the interfacial tension between the nanoparticle and the A or B segment of the block copolymer. Haryono and Binder[16] reported that the interfacial energy between nanoparticle and polymer segment is $\Delta\gamma = \gamma_{A-B}$, so that $|\cos\theta_{A-B}| \ll 1$ and $E_a \approx \pi R^2 \gamma_{A-B}$. Because the Au-1k nanoparticles are located at the interfaces of microdomains, the enthalpic effect is important for discussing their localization. The surface tensions of PS, PI and PMMA are 40.7, 32.0 and 41.1 mN m^{-1}, respectively.[48] Because $\gamma_{PS-PI} > \gamma_{PS-PMMA}$, E_a is larger when the Au-1k nanoparticles are located at the interface between PS and PI than when the nanoparticles are located at the interface between PS and PMMA. Therefore, the nanoparticles selectively absorb at the PS/PI interfaces (Figure 4c). The localization of the three types of Au nanoparticles are successfully explained by the entropic and enthalpic energies between the Au nanoparticles and SIM.

Table 3 Size relationships between PS-grafted Au nanoparticles and SIM

Au nanoparticle	D/L	r_{PS}	*Wet or dry brush*[a]
Au-11k	0.53	1.2	Dry brush
Au-3k	0.27	0.44	Wet brush
Au-1k	0.21	0.22	Wet brush

Abbreviations: PS, polystyrene; SIM, poly(styrene-*b*-isoprene-*b*-methyl methacrylate).
$r_{PS} = \frac{r_{PS-NPs}}{r_{PS-block}} = \frac{N_{PS-homo}}{N_{PS-block}}$, where $N_{PS-homo}$ and $N_{PS-block}$ are polymerization degrees of PS homopolymer and PS block in SIM, respectively.
When $r_{PS} \geqslant 1.0$, Au nanoparticles are blended like a dry brush.
[a]When $r_{PS} < 1.0$, Au nanoparticles are blended like a wet brush.

The distributions of Au-11k and Au-3k nanoparticles in the microdomains were similar to those from the prediction based on the wet and dry brush theory.[49,50] The PS-grafted Au nanoparticles are not PS homopolymers but were assumed to have the same size as PS molecules (r_{PS-NPs}) to discuss the morphological transition by incorporating the Au nanoparticles as:

$$D \simeq r_{PS-NPs} \quad (2)$$

$$r_{PS} = \frac{r_{PS-NPs}}{r_{PS-block}} = \frac{N_{PS-homo}}{N_{PS-block}} \quad (3)$$

where $r_{PS\text{-}block}$ is the size of PS block in SIM, $N_{PS\text{-}homo}$ and $N_{PS\text{-}block}$ are polymerization degrees of PS homopolymer, which is estimated as the Gaussian chain with same-sized PS molecules to *D*, and PS block in SIM, respectively. The sizes of Au nanoparticles approximated as PS molecules are summarized in Table 3. When $r_{PS} \geqq 1$, the PS-grafted nanoparticles are localized at the center of the PS microdomain (dry brush regime), where the nanoparticles are unperturbed by the surrounding PS segments of SIM. It is also assumed that the nanoparticles weakly affect the chain conformation of the PS segments. However, the nanoparticles are uniformly distributed in the PS microdomain when $r_A < 1$ (wet brush regime) and affect the chain conformation of the PS segments. The r_{PS} value of the Au-11k nanoparticles was calculated as 1.2, indicating that the Au-11k nanoparticles were incorporated in the dry brush regime (Figure 4a). The Au-11k nanoparticles were located at the center of the PS domains and did not affect the chain conformation of the PS segments of SIM. Thus, even though the Au-11k nanoparticles were incorporated at high concentrations, the SIM molecules retained the same chain conformation in bulk and the morphology was transformed to a lamellar structure by the volume increase of the PS phase. However, the r_{PS} value of Au-3k nanoparticles was calculated as 0.44, indicating that the incorporated Au-3k nanoparticles were under the wet brush regime (Figure 4b). The Au-3k nanoparticles affect the chain conformation of the PS segments of SIM, and hence when the nanoparticles were incorporated at high concentration, the microphase-separated structure became disordered and the nanoparticles were macroscopically separated.

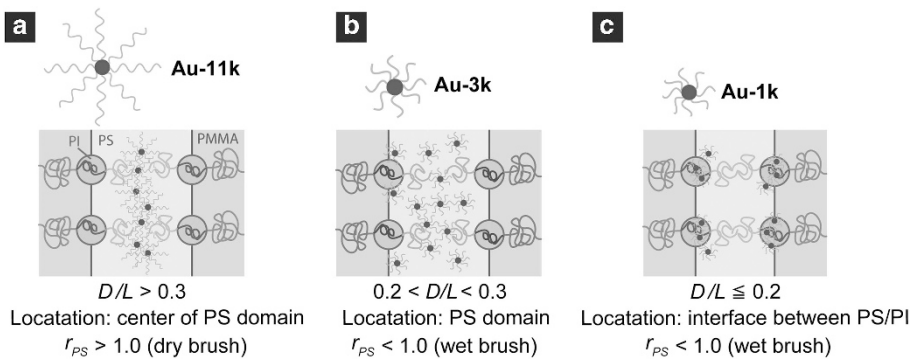

Figure 4 Schematic illustration of incorporation behaviors of (**a**) Au-11k, (**b**) Au-3k and (**c**) Au-1k nanoparticles into the poly(styrene-*b*-isoprene-*b*-methyl methacrylate) (SIM) microdomains. A full color version of this figure is available at *Polymer Journal* online.

CONCLUSION

In this study, we demonstrated the controlled incorporation of Au nanoparticles grafted with PS molecules in the helical microdomains of ABC-type linear triblock terpolymers composed of PS, PI and PMMA. The Au nanoparticles grafted with three PSs with different molecular weights were synthesized and incorporated into the SIM films. The morphologies of composite films and localization of Au nanoparticles were 3D characterized with TEMT observation. TEMT structural analysis revealed that the PS-grafted Au nanoparticles, whose size is >0.3 times the respective domain dimension of PS microdoamin in SIM, were located at the interfaces of PS microdoamins to minimize the entropy loss of the PS segment of SIM. In contrast, Au nanoparticles <0.2 times the respective domain dimension were located at the interface of PS and PI microdomain to reduce the interfacial tension between the nanoparticles and SIM. The intermediate-sized Au nanoparticles were uniformly distributed in the PS microdomains. When the incorporating ratio of Au nanoparticles exceeded the limit, the helical microdomains of SIM were transformed to lamellar structures to retain their chain conformation in the case of Au nanoparticles with PS molecules having a higher molecular weight than that of PS segment of SIM. In contrast, when the Au nanoparticles with PS molecules had a lower molecular weight than that of PS segment of SIM, the microphase-separated structures were transformed to the disordered structure.

CONFLICT OF INTEREST

The authors declare no conflict of interest.

ACKNOWLEDGEMENTS

We are grateful to Mr Kazutaka Koike of IMRAM, Tohoku University, for helping in the synthesis of gold nanoparticles. We also acknowledge Mr Yosuke Sawayama of Sumitomo Bakelite Co., Ltd. for helping in the TEMT observation. This work has been partially supported by JSPS KAKENHI (Grant Numbers 25706006 and 26620171, Japan).

1 Khandpur, A. K., Förster, S., Bates, F. S., Hamley, I. W., Ryan, A. J., Bras, W., Almdal, K. & Mortensen, K. Polyisoprene-polystyrene diblock copolymer phase diagram near the order-disorder transition. *Macromolecules* **28**, 8796–8806 (1995).
2 Jinnai, H., Nishikawa, Y., Spontak, R. J., Smith, S. D., Agard, D. A. & Hashimoto, T. Direct measurement of interfacial curvature distributions in a bicontinuous block copolymer morphology. *Phys. Rev. Lett.* **84**, 518–521 (2000).
3 Alward, D., Kinning, D., Thomas, E. & Fetters, L. Effect of arm number and arm molecular-weight on the solid-state morphology of poly(styrene-isoprene) star block copolymers. *Macromolecules* **19**, 215–224 (1986).
4 Matyjaszewski, K., Miller, P., Pyun, J., Kickelbick, G. & Diamanti, S. Synthesis and characterization of star polymers with varying arm number, length, and composition from organic and hybrid inorganic/organic multifunctional initiators. *Macromolecules* **32**, 6526–6535 (1999).
5 Börner, H., Beers, K., Matyjaszewski, K., Sheiko, S. & Moller, M. Synthesis of molecular brushes with block copolymer side chains using atom transfer radical polymerization. *Macromolecules* **34**, 4375–4383 (2001).
6 Higaki, Y., Otsuka, H. & Takahara, A. Synthesis of well-defined poly(styrene)-b-poly(p-tert-butoxystyrene) multiblock copolymer from poly(alkoxyamine) macroinitiator. *Polymer* **44**, 7095–7101 (2003).
7 Lee, S. B., Russell, A. J. & Matyjaszewski, K. Atrp synthesis of amphiphilic random, gradient, and block copolymers of 2-(dimethylamino)ethyl methacrylate and n-butyl methacrylate in aqueous media. *Biomacromolecules* **4**, 1386–1393 (2003).
8 Okabe, S., Seno, K., Kanaoka, S., Aoshima, S. & Shibayama, M. Micellization study on block and gradient copolymer aqueous solutions by dls and sans. *Macromolecules* **39**, 1592–1597 (2006).
9 Yang, S., Ryu, I., Kim, H., Kim, J., Jang, S. & Russell, T. P. Nanoporous membranes with ultrahigh selectivity and flux for the filtration of viruses. *Adv. Mater.* **18**, 709–712 (2006).
10 Edrington, A. C., Urbas, A. M., DeRege, P., Chen, C. X., Swager, T. M., Hadjichristidis, N., Xenidou, M., Fetters, L. J., Joannopoulos, J. D. & Fink, Y. Polymer-based photonic crystals. *Adv. Mater.* **13**, 421–425 (2001).
11 Kang, Y., Walish, J. J., Gorishnyy, T. & Thomas, E. L. Broad-wavelength-range chemically tunable block-copolymer photonic gels. *Nat. Mater.* **6**, 957–960 (2007).
12 Yoon, J., Lee, W. & Thomas, E. L. Optically pumped surface-emitting lasing using self-assembled block-copolymer-distributed bragg reflectors. *Nano Lett.* **6**, 2211–2214 (2006).
13 Park, M., Harrison, C., Chaikin, P. M., Register, R. A. & Adamson, D. H. Block copolymer lithography: periodic arrays of 1011 holes in 1 square centimeter. *Science* **276**, 1401–1404 (1997).
14 Jeong, S.-J., Moon, H.-S., Kim, B. H., Kim, J. Y., Yu, J., Lee, S., Lee, M. G., Choi, H. & Kim, S. O. Ultralarge-area block copolymer lithography enabled by disposable photoresist prepatterning. *ACS Nano* **4**, 5181–5186 (2010).
15 Shenhar, R., Norsten, T. B. & Rotello, V. M. Polymer-mediated nanoparticle assembly: Structural control and applications. *Adv. Mater.* **17**, 657–669 (2005).
16 Haryono, A. & Binder, W. H. Controlled arrangement of nanoparticle arrays in block-copolymer domains. *Small* **2**, 600–611 (2006).
17 Lopes, W. A. & Jaeger, H. M. Hierarchical self-assembly of metal nanostructures on diblock copolymer scaffolds. *Nature* **414**, 735–738 (2001).
18 Tsutsumi, K., Funaki, Y., Hirokawa, Y. & Hashimoto, T. Selective incorporation of palladium nanoparticles into microphase-separated domains of poly(2-vinylpyridine)-block-polyisoprene. *Langmuir* **15**, 5200–5203 (1999).
19 Lauter-Pasyuk, V., Lauter, H. J., Ausserre, D., Gallot, Y., Cabuil, V., Kornilov, E. I. & Hamdoun, B. Effect of nanoparticle size on the internal structure of copolymer-nanoparticles composite thin films studied by neutron reflection. *Physica B.* **241-243**, 1092–1094 (1997).
20 Bronstein, L. M., Sidorov, S. N., M, V. P., Hartmann, J., Cölfen, H. & Antonietti, M. Induced micellization by interaction of poly(2-vinylpyridine)-block-poly(ethylene oxide) with metal compounds. micelle characteristics and metal nanoparticle formation. *Langmuir* **15**, 6256–6262 (1999).
21 Zhang, Q., Xu, T., Butterfield, D., Misner, M. J., Ryu, D. Y., Emrick, T. & Russell, T. P. Controlled placement of cdse nanoparticles in diblock copolymer templates by electrophoretic deposition. *Nano Lett.* **5**, 357–361 (2005).
22 Chiu, J. J., Kim, B. J., Kramer, E. J. & Pine, D. J. Control of nanoparticle location in block copolymers. *J. Am. Chem. Soc.* **127**, 5036–5037 (2005).
23 Mayeda, M. K., Kuan, W.-F., Young, W.-S., Lauterbach, J. A. & Epps, T. H. III Controlling particle location with mixed surface functionalities in block copolymer thin films. *Chem. Mater.* **24**, 2627–2634 (2012).
24 Lin, Y., Böker, A., He, J., Sill, K., Xiang, H., Abetz, C., Li, X., Wang, J, Emrick, T., Long, S., Wang, Q., Balazs, A. & Russell, T. P. Self-directed self-assembly of nanoparticle/copolymer mixtures. *Nature* **434**, 55–59 (2005).
25 Yabu, H., Jinno, T., Koike, K., Higuchi, T. & Shimomura, M. Nanoparticle arrangements in block copolymer particles with microphase-separated structures. *J. Polym. Sci. Polym. Phys.* **49**, 1717–1722 (2011).
26 Yabu, H., Jinno, T., Koike, K., Higuchi, T. & Shimomura, M. Three-dimensional assembly of gold nanoparticles in spherically confined microphase-separation structures of block copolymers. *Macromolecules* **44**, 5868–5873 (2011).
27 Auschra, C. & Stadler, R. New ordered morphologies in ABC triblock copolymers. *Macromolecules* **26**, 2171–2174 (1993).
28 Krappe, U., Stadler, R. & Voigt-Martin, I. Chiral assembly in amorphous ABC triblock copolymers - formation of a helical morphology in polystyrene-block-polybutadiene-block-poly(methyl methacrylate) block-copolymers. *Macromolecules* **28**, 7583–7583 (1995).
29 Abetz, V. & Goldacker, T. Formation of superlattices via blending of block copolymers. *Macromol. Rapid Commun.* **21**, 16–34 (2000).
30 Schacher, F., Yuan, J., Schoberth, H. G. & Müller, A. H. E. Synthesis, characterization, and bulk crosslinking of polybutadiene-block-poly(2-vinyl pyridine)-block-poly(tert-butyl methacrylate) block terpolymers. *Polymer* **51**, 2021–2032 (2010).
31 Li, Z., Hur, K., Sai, H., Higuchi, T., Takahara, A., Jinnai, H., Gruner, S. M. & Wiesner, U. Linking experiment and theory for three-dimensional networked binary metal nanoparticle–triblock terpolymer superstructures. *Nat. Commun.* **5**, 3247 (2014).
32 Gansel, J. K., Thiel, M., Rill, M. S., Decker, M., Bade, K., Saile, V., von Freymann, G., Linden, S. & Wegener, M. Gold helix photonic metamaterial as broadband circular polarizer. *Science* **325**, 1513–1515 (2009).
33 Jinnai, H., Kaneko, T., Matsunaga, K., Abetz, C. & Abetz, V. A double helical structure formed from an amorphous, achiral abc triblock terpolymer. *Soft Matter* **5**, 2042–2046 (2009).
34 Higuchi, T., Sugimori, H., Jiang, X., Hong, S., Matsunaga, K., Kaneko, T., Abetz, V., Takahara, A. & Jinnai, H. Morphological control of helical structures of an ABC-type triblock terpolymer by distribution control of a blending homopolymer in a block copolymer microdomain. *Macromolecules* **46**, 6991–6997 (2013).
35 Kawase, N., Kato, M., Nishioka, H. & Jinnai, H. Transmission electron microtomography without the 'missing wedge' for quantitative structural analysis. *Ultramicroscopy* **107**, 8–15 (2007).
36 Jinnai, H., Spontak, R. J. & Nishi, T. Transmission electron microtomography and polymer nanostructures. *Macromolecules* **43**, 1675–1688 (2010).
37 Jinnai, H., Tsuchiya, T., Motoki, S., Kaneko, T., Higuchi, T. & Takahara, A. Transmission electron microtomography in soft materials. *Microscopy* **62**, 243–258 (2013).
38 Hong, S., Higuchi, T., Sugimori, H., Kaneko, T., Abetz, V., Takahara, A. & Jinnai, H. Highly oriented and ordered double-helical morphology in abc triblock terpolymer films up to micrometer thickness by solvent evaporation. *Polym. J.* **44**, 567–572 (2012).
39 Brust, M., Walker, M., Bethell, D., Schiffrin, D. J. & Whyman, R. Synthesis of thiol-derivatised gold nanoparticles in a two-phase liquid–liquid system. *J. Chem. Soc. Chem. Commun.* 801–802 (1994).

40 Crowther, R. A., DeRosier, D. J. & Klug, A. The reconstruction of a three-dimensional structure from projections and its application to electron microscopy. *Proc. R. Soc. A* **317**, 319–340 (1970).
41 Yockell-Lelievre, H., Desbiens, J. & Ritcey, A. M. Two-dimensional self-organization of polystyrene-capped gold nanoparticles. *Langmuir* **23**, 2843–2850 (2007).
42 Thompson, R. B., Ginzburg, V. V., Matsen, M. W. & Balazs, A. C. Predicting the mesophases of copolymer-nanoparticle composites. *Science* **292**, 2469–2472 (2001).
43 Spontak, R. J., Shankar, R., Bowman, M. K., Krishnan, A. S., Hamersky, M. W., Samseth, J., Bockstaller, M. R. & Rasmussen, K. Ø. Selectivity- and size-induced segregation of molecular and nanoscale species in microphase-ordered triblock copolymers. *Nano Lett.* **6**, 2115–2120 (2006).
44 Kim, B. J., Bang, J., Hawker, C. J. & Kramer, E. J. Effect of areal chain density on the location of polymer-modified gold nanoparticles in a block copolymer template. *Macromolecules* **39**, 4108–4114 (2006).
45 Kim, B. J., Fredrickson, G. H. & Kramer, E. J. Effect of polymer ligand molecular weight on polymer-coated nanoparticle location in block copolymers. *Macromolecules* **41**, 436–447 (2008).
46 Bockstaller, M. R., Lapetnikov, Y., Margel, S. & Thomas, E. L. Size-selective organization of enthalpic compatibilized nanocrystals in ternary block copolymer/particle mixtures. *J. Am. Chem. Soc.* **125**, 5276–5277 (2003).
47 Pieranski, P. Two-dimensional interfacial colloidal crystals. *Phys. Rev. Lett.* **45**, 569–572 (1980).
48 Brandrup, J., Immergut, E. H. & Grulke, E. A. *Polymer Handbook,* Vol. 1-2, (John Wiley & Sons Inc., Weinheim, Germany, 1999).
49 Hashimoto, T., Tanaka, H. & Hasegawa, H. Ordered structure in mixtures of a block copolymer and homopolymers. 2. Effect of molecular weights of homopolymers. *Macromolecules* **23**, 4378–4386 1990).
50 Koizumi, S., Hasegawa, H. & Hashimoto, T. Ordered structure of block copolymer/homopolymer mixtures. 5. Interplay of macro- and microphase transitions. *Macromolecules* **27**, 6532–6540 (1994).

Supplementary Information accompanies the paper on Polymer Journal website (http://www.nature.com/pj)